MIXED CONVECTION FLOW AND HEAT TRANSFER IN FERROMAGNETIC FLUID OVER A STRETCHING SHEET WITH PARTIAL SLIP EFFECTS

by

Ahmad ZEESHAN[a], Aaqib MAJEED[b], Rahmat ELLAHI[c,a*], and Qazi Muhammad Zaigham ZIA[d]

[a] Department of Mathematics and Statistics, FBAS, IIUI, Islamabad, Pakistan
[b] Bacha Khan University Charsadda, KPK, Pakistan
[c] Center for Modeling & Computer Simulation, Research Institute, King Fahd University of Petroleum & Minerals, Dhahran, Saudi Arabia
[d] Department of Mathematics, COMSATS Institute of Information Technology Islamabad, Pakistan

Original scientific paper
https://doi.org/10.2298/TSCI160610268Z

The 2-D steady boundary layer mixed convection flow and heat transfer in ferromagnetic fluid over a stretching sheet is investigated. Velocity slip is taken into account. The governing partial differential equations are first transformed into the non-linear ordinary coupled differential equation using a similarity transformation and then solved numerically by Runge-Kutta-Fehlberg method. The role of local skin friction, heat transfer rate, ferromagnetic-interaction parameter, slip parameter and the buoyancy parameter on velocity and temperature profiles inside the boundary layers are examined through tables and graphically. Finally a comparison is also made with the existing literature and found in good agreement.

Key words: *ferromagnetic interaction parameter, partial slip, buoyancy parameter, magnetic dipole, numerically*

Introduction

The incompressible viscous fluid past a stretching sheet has become a classical problem in fluid dynamics as it admits an unusual simple closed form solution, first discovered by Crane [1]. This problem was then extended to a permeable surface by Gupta and Gupta [2]. Later on Grubka and Bobba [3] have considered a more general case with power law surface temperature variation. They reported a series solution to the energy equation in terms of Kummer's functions and presented several closed-form analytical solutions for specific conditions. Such type of non-Newtonian viscous fluid can be found in [4-6]. Recent trends in non-Newtonian ferrofluids have led to develop a new innovative class of heat transfer called nanofluids created by dispersing nanoparticles in traditional heat transfer fluids. In fact ferrofluids are non-conducting stable suspensions of colloidal ferromagnetic particles, with typical dimensions of about 10 to100 nm, dispersed in nanofluid [7-15]. These colloidal particles are coated with surfactants to avoid their agglomeration. Because of the industrial applications of ferrofluids is to attract the researchers and engineers dynamically since last five decades. Ferrofluids are a unique class of material, not freely available in nature, but are to be synthesized. A typical ferrofluid

* Corresponding author, e-mail: rellahi@alumni.ucr.edu, rahmatellahi@yahoo.com

may contain 5% magnetic solid, 10% surfactant, and 85% carrier. These fluids have a variety of applications in the field of mechanical, electrical and electronics engineering. Ferrofluids are widely used in rotating shafts and rods, rotating X-ray tubes and sealing of computer hard disk. These are also utilized as lubricants in bearing and dumpers. Ferrofluids are also used to control the heat in hi-fi speaker and electric motors systems without modifying their geometry [16]. Ferrofluids are being greatly used in many magnetic fluids based scientific devices like sensor, accelerometer, densimeters, pressure transducers, *etc.* Also in actuating mechanism like electromechanical converters and energy converter analyzed by Raj and Moskowitz [17]. Ferrofluids are also used for treating cancer by heating the tumour soaked in ferrofluids by means of alternating magnetic fields [18-20]. The convincing introduction to the researcher on magnetic liquids and interesting information on the study of magnetization is given by Rosensweing *et al*. [21]. Later Neuringer [22] worked on saturated ferrofluids under the influence of thermal and magnetic field gradients. Under the action of magnetic fluid convective boundary layer flow of a magnetic fluid over a plate was considered by Tzirtzilakis *et al*. [23]. Sheikholeslami and Ellahi [24] reported the simulation of ferrofluid flow for magnetic drug targeting using Lattice Boltzmann method. Sheikholeslami and Gorji [25] gave a numerical solution of free convection ferrofluid in a cavity heated from below in the presence of external magnetic using the Lattice Boltzmann method. Li and Xuan [26] exhibited the experiments on the ferrofluid flow over fine wire and found that external magnetic field affects the performance of convective heat transfer of the magnetic fluids. They found that the external magnetic field affects the convective heat transfer performances of the magnetic fluids. Motozawa *et al*. [27] investigated experimentally the effect of magnetic field on heat transfer in rectangular duct flow. Feng *et al*. [28] presented an experimental study in the presence of external magnetic field for controlling the acoustically heat transfer of a ferromagnetic fluid. Tangthieng *et al*. [29] performed the finite element simulations of heat transfer to a ferrofluid in the presence of a magnetic field. Stiles *et al*. [30] have analyzed linear and weakly nonlinear thermoconvective instability in a thin layer of ferrofluid subject to a weak external magnetic field in the vertical direction.

Moreover, the study of boundary layer flow and heat transfer over a stretching surface is important due to its numerous applications in engineering and manufacturing process in industry like aerodynamic extrusion of plastic sheets, paper production, glass fiber production, heat treated materials traveling between a feed roll and a wind-up roll in the polymer industry, wires drawing, metal spinning, and many others [31-34]. Furthermore, Hayat *et al*. [35] obtained analytical solution of the slip flow and heat transfer of a second grade fluid past a planar stretching sheet. Martin and Boyd [36] have examined the slip flow and heat transfer past a flat surface at constant wall temperature. Their results demonstrate that the boundary layer equations can be used to study flow at micro-electromechanical systems (MEMS) scale and provide useful information to study the effects of rarefaction on the shear stress and structure of the flow. For more detail on slip readers are referred to see [37] and several references therein. Additionally, it is also an established fact that when the differences of harmonious order between free convection and forced differences occurs then the mixed convection gets up. It has energetic entry in atmospheric boundary layer flows, solar collectors, heat exchangers, electronic equipment's, *etc.* Mixed convectional flow with heat transfer is extensively used in chemical industries like nuclear reactor cooling system and design of canisters for nuclear waste disposal. These physical processes happen in the situation when the impacts of buoyancy forces become much more dominant. Ali [38] has studied the effect of temperature dependent viscosity on laminar mixed convection heat transfer along a continuous moving surface. Hayat *et al*. [39] analysed the effect of Soret and Dufour effect on mixed convection flow over a vertical stretching

surface in the presence of porous medium filled with a viscoelastic fluid. Some relevant studies on mixed convection can be found in [40-44].

In the previous view, the present paper examines the effects of mixed convection flow and heat transfer in ferromagnetic particle past a stretching surface in the presence of partial slip. The governing partial differential equations are reduced into ordinary differential equations by introducing appropriate similarity transformations. These highly non-linear ordinary differential equations are solved numerically using Runge-Kutta-Fehlberg method with the help of MATLAB. Further the effect of some physical parameter like buoyancy parameter, Prandtl number, ferromagnetic interaction parameter on velocity and temperature profile are analyzed.

Mathematical formulation

Consider a 2-D study of an incompressible ferromagnetic fluid electrically non-conducting past a stretching sheet which is placed in the plane $y = 0$, with linear velocity $u_w = cx$, where $c > 0$ is the stretching rate as shown schematically in fig. 1. The flow is being confined by $y > 0$. Two equal and opposite forces are introduced along the x-axis so that wall is stretched while keeping the origin fixed with a velocity u_w which is proportional to the distance from the origin. A magnetic dipole is located with its centre on the y-axis is at a distance a from the sheet. The magnetic field due to the dipole points in the positive x-direction giving rise to a magnetic field of sufficient strength to saturate the ferrofluid. It is also assumed that the uniform temperature at the surface of the sheet is T_w and Curie temperature T_c, while the temperature of the ambient ferrofluid far from the surface of the sheet are $T_\infty = T_c$ and hence unable to magnetized until they start to cool after entering the thermal boundary layer region adjacent to the sheet.

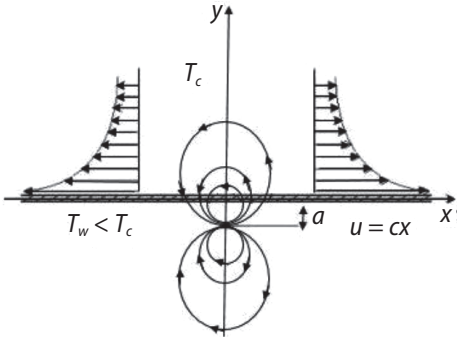

Figure 1. Schematic representation of flow configuration; circles represent the magnetic field

The governing boundary layer equations for flow and heat transfer are:

$$\frac{\partial u}{\partial x} + \frac{\partial v}{\partial y} = 0 \tag{1}$$

$$\rho\left(u\frac{\partial u}{\partial x} + v\frac{\partial u}{\partial y}\right) = -\frac{\partial p}{\partial x} + \mu_0 M\frac{\partial M}{\partial x} + \mu\left(\frac{\partial^2 u}{\partial x^2} + \frac{\partial^2 u}{\partial y^2}\right) + g\beta^*(T_c - T) \tag{2}$$

$$\rho\left(u\frac{\partial v}{\partial x} + v\frac{\partial v}{\partial y}\right) = -\frac{\partial p}{\partial y} + \mu_0 M\frac{\partial M}{\partial y} + \mu\left(\frac{\partial^2 v}{\partial x^2} + \frac{\partial^2 v}{\partial y^2}\right) + g\beta^*(T_c - T) \tag{3}$$

$$\rho c_p\left(u\frac{\partial T}{\partial x} + v\frac{\partial T}{\partial y}\right) + \mu_0 T\frac{\partial M}{\partial T}\left(u\frac{\partial H}{\partial x} + v\frac{\partial H}{\partial y}\right) = k\frac{\partial^2 T}{\partial y^2} + \mu\left[2\left(\frac{\partial u}{\partial x}\right)^2 + 2\left(\frac{\partial v}{\partial y}\right)^2 + \left(\frac{\partial v}{\partial x} + \frac{\partial u}{\partial y}\right)^2\right] \tag{4}$$

where u and v and are the velocity components along the x- and y-directions, respectively. The T is the fluid temperature, ρ – the density of the fluid, μ – the dynamic viscosity, $\nu = \mu/\rho$ – the kinematic viscosity, μ_0 – the magnetic permeability, k – the thermal conductivity, c_p –

specific heat, g – the acceleration due to gravity, β^* – the volumetric coefficient of thermal expansion, M – the magnetization, and H – the magnetic field. The term $\mu_0 M(\partial M/\partial x)$ and $\mu_0 M(\partial M/\partial y)$ in eqs. (2) and (3), represent the components of the ferromagnetic force per unit volume and depend on the existence of the magnetic gradient. In the absence of magnetic gradient these forces will be disappeared. The second term, in eq. (4) on the left-hand side represent the heating due to adiabatic magnetization.

The boundary conditions for the flow problem are:

$$u = u_w + A\frac{\partial u}{\partial y}, \quad v = 0, \quad T = T_w = T_c - D\left(\frac{x}{l}\right)^2 \quad \text{at} \quad y = 0 \tag{5}$$

$$u = 0, \quad T = T_c, \quad p + \frac{1}{2}\rho(u^2 + v^2) = \text{constant} \quad \text{as} \quad y \to \infty \tag{6}$$

where A is the velocity slip factor, D – a positive constant, and $l = (\nu/c)^{1/2}$ – the characteristic length. The flow of ferrofluid is affected by the magnetic field due to the magnetic dipole whose magnetic scalar potential is given:

$$\Phi = \frac{\gamma}{2\pi}\left[\frac{x}{x^2 + (y+a)^2}\right] \tag{7}$$

where γ is the magnetic field strength at the source. The components of magnetic field intensity H_x and H_y along the x- and y-axes are given:

$$H_x = -\frac{\partial \Phi}{\partial x} = \frac{\alpha}{2\pi}\left(\left\{\frac{x^2 - (y+a)^2}{\left[x^2 + (y+a)^2\right]^2}\right\}\right) \tag{8}$$

$$H_y = -\frac{\partial \Phi}{\partial y} = \frac{\alpha}{2\pi}\left(\left\{\frac{2x(y+a)}{\left[x^2 + (y+a)^2\right]^2}\right\}\right) \tag{9}$$

Since the magnetic body force is proportional to the gradient of the magnitude of H. The resultant magnitude H of the magnetic field intensity, after having expanded in powers of x and retained terms up to order x^2, is given by:

$$H = \left[\left(\frac{\partial \Phi}{\partial x}\right)^2 + \left(\frac{\partial \Phi}{\partial y}\right)^2\right]^{\frac{1}{2}} \tag{10}$$

$$\frac{\partial H}{\partial x} = -\frac{\gamma}{2\pi}\left[\frac{2x}{(y+a)^4}\right] \tag{11}$$

$$\frac{\partial H}{\partial y} = \frac{\gamma}{2\pi}\left[\frac{-2}{(y+a)^3} + \frac{4x^2}{(y+a)^5}\right] \tag{12}$$

Andersson and Valnes [45] considered that the variation of magnetization M can be approximated, as a function of temperature T by the linear equation:

$$M = K^*(T_c - T) \tag{13}$$

where K^* is a constant called pyromagnetic coefficient and T_c is the Curie temperature, however, the appearance of ferrohydrodynamic interaction requires that: (1) the fluid is at a temperature T different from T_c and (2) the applied magnetic field is inhomogeneous. When the ferrofluid reaches the Curie temperature, it is no longer subjected to further magnetization. This feature is essential for physical applications because the Curie temperature is very high, *e. g.* 1043 K for iron.

Solution procedure

We introduce the non-dimensional variables assumed by Andersson and Valnes [45]:

$$\Psi(\xi,\eta)=\left(\frac{\mu}{\rho}\right)\xi f(\eta) \tag{14}$$

$$P(\xi,\eta)\equiv\frac{p}{c\mu}=-P_1(\eta)-\xi^2P_2(\eta) \tag{15}$$

$$\theta(\xi,\eta)\equiv\frac{T_c-T}{T_c-T_w}=\theta_1(\eta)+\xi^2\theta_2(\eta) \tag{16}$$

where $T_c-T_w=D(x/l)^2$ and ξ,η are the dimensionless co-ordinates defined:

$$\xi=\sqrt{\frac{c\rho}{\mu}}x,\quad \eta=\sqrt{\frac{c\rho}{\mu}}y \tag{17}$$

and $\Psi(\xi,\eta)$ and $\theta(\xi,\eta)$ are the dimensionless stream function and temperature, respectively. The velocity components can be calculated:

$$u=\frac{\partial\Psi}{\partial y}=cxf'(\eta),\quad v=-\frac{\partial\Psi}{\partial x}=-\sqrt{c\nu}\,f(\eta) \tag{18}$$

Substituting eqs. (14)-(18) into the eqs. (2)-(4) and equating coefficients of like powers of ξ, up to ξ^2, we obtain the following system of ordinary differential equations:

$$\begin{aligned}
&f'''+ff''-f'^2-\frac{2\beta\theta_1}{(\eta+\alpha_1)^4}+2P_2+G^*\theta_1=0\\
&P_1'-f''-ff'-\frac{2\beta\theta_1}{(\eta+\alpha_1)^3}+G^*\theta_1=0\\
&P_2'-\frac{2\beta\theta_2}{(\eta+\alpha)^3}+\frac{4\beta\theta_1}{(\eta+\alpha_1)^5}+G^*\theta_2=0\\
&\theta_1''-\Pr(2f'\theta_1-f\theta_1')+\frac{2\lambda\beta(\theta_1-\varepsilon)f}{(\eta+\alpha_1)^3}-4\lambda(f')^2=0\\
&\theta_2''-\Pr(4f'\theta_2-f\theta_2')-\lambda\beta(\theta_1-\varepsilon)\left[\frac{2f'}{(\eta+\alpha_1)^4}+\frac{4f}{(\eta+\alpha_1)^5}\right]+\frac{2\lambda\beta f\theta_2}{(\eta+\alpha_1)^3}-\lambda(f'')^2=0
\end{aligned} \tag{19}$$

Also the boundary conditions (5) and (6) are transformed:

$$f=0,\quad f'=1+\delta f''(0),\quad \theta_1=1,\quad \theta_2=0,\quad \text{at}\quad \eta=0 \tag{20}$$

$$f' \to 0, \quad \theta_1 \to 0, \quad \theta_2 \to 0, \quad P_1 \to -P_\infty, \quad P_2 \to 0 \quad \text{as} \quad \eta \to \infty \tag{21}$$

The dimensionless parameters appearing in the transformed eqs. (19) and (20) are:

$$\begin{gathered} \beta = \frac{\gamma\rho}{2\pi\mu^2}\mu_0 K^*\left(T_c - T_w\right), \quad G^* = \frac{Gr_x}{\mathrm{Re}_x^2}, \quad \mathrm{Gr}_x = \frac{\mathrm{g}\beta^*(T_c - T_w)}{\nu^2}, \quad \delta = A\sqrt{\frac{c}{\nu}} \\ \lambda = \frac{c\mu^2}{\rho k\left(T_c - T_w\right)}, \quad \alpha_1 = \sqrt{\frac{c\rho}{\mu}}a, \quad \mathrm{Pr} = \frac{\mu c_p}{k}, \quad \varepsilon = \frac{T_c}{T_c - T_w} \end{gathered} \tag{22}$$

where β is the ferromagnetic interaction parameter, $G^* \geq 0$ – the buoyancy or mixed convection parameter, Gr_x – the local Grashof number, δ – the velocity slip parameter, λ – the viscous dissipation parameter, α_1 – dimensionless distance, Pr – the Prandtl number, and ε – the dimensionless Curie temperature ratio.

The most important physical quantities of practical interest are the local skin friction coefficient C_{f_x} and the local rate of heat transfer coefficient Nu_x can be written:

$$C_{f_x} = \frac{-2\tau_w}{\rho\left(cx\right)^2}, \quad \mathrm{Nu}_x \equiv \frac{xq_w}{-k\left(T_c - T_w\right)} \tag{23}$$

in which shear stress, τ_w, and heat flux, q_w, are defined:

$$\tau_w = \mu\left(\frac{\partial u}{\partial y}\right)_{y=0}, \quad q_w = -\left(\frac{\partial T}{\partial y}\right)_{y=0} \tag{24}$$

using the equations (14)-(18) we have

$$C_f\,\mathrm{Re}_x^{1/2} = -2f''(0), \qquad \frac{\mathrm{Nu}_x}{\mathrm{Re}_x^{1/2}} = -\left[\theta_1'(0) + \xi^2\theta_2'(0)\right] \tag{25}$$

where $f''(0)$ is the dimensionless wall shear parameter, $\theta_1'(0)$ – the dimensionless heat transfer rate at sheet, $\mathrm{Re}_x = \rho cx^2/\mu$ – the local Reynolds number. It is apparent that the flow field is affected by the ferromagnetic interaction parameter β. It is more interesting and convenient to replace the dimensionless wall heat transfer parameter $-\theta_1' = -[\theta_1'(0) + \xi^2\theta_2'(0)]$ by the dimensionless and independent of the distance ξ, ratio $\theta^*(0) = \theta_1'(0)/[\theta_1'(0)|_{\beta=0}]$ called the coefficient of the heat transfer rate at the sheet.

Numerical results and discussion

The effects of various physical parameter namely, the ferromagnetic interaction parameter, β, buoyancy parameter, G^*, partial slip parameter, δ, Prandtl number, Pr, on the flow and heat transfer is ferromagnetic fluid are illustrated in this section with the help of figures and tables.

The transformed differential eq. (19) together with boundary conditions (20) and (21) are highly non-linear and cannot be solved analytically and must solved numerically by shooting method. The higher-order ODE are converted into the set of seven first-order simultaneous equations, which can be integrated as an initial value problem using the efficient Runge-Kutta Fehlberg fourth-order technique. The step-size is taken as $\nabla\eta = 0.01$. Trial values of $f''(0)$, $\theta_1'(0)$, $\theta_2'(0)$, and $P_2(0)$ were adjusted iteratively by Newton-Raphsons' method in order to satisfy the far field boundary condition, *i. e.* at $\eta \to \infty$ is satisfied at a finite value. The maximum value of η_∞ is equal to 10.

It is well known fact that slip effects appear for two types of fluids namely, rare field gases fluids having much more elastic character. It is detected through experiment observations that the existence of slippage has important role in polymer, molten polymer solutions and the polishing of artificial heart valves and internal cavities as well. Keeping the importance of slip in mind the velocity and temperature profiles for different value of the physical parameters have been presented in figs. 2-8. Figure 2 and 3 show the velocity and temperature distributions with different values of the velocity slip parameter δ. It is clear from fig. 2 that the velocity decreases in the presence of slip at the fluid-solid interface and decreases monotonically to zero far away from the solid surface. In case of the no-slip condition, the fluid velocity adjacent to the solid surface is equal to the velocity of the stretching sheet, then $f'(0)=1$, which is clearly satisfied in this figure. Figure 3 indicates that an increase in the velocity slip δ parameter tends to increase the temperature of the fluid and consequently decrease the temperature gradient, which represents the rate of heat transfer. This observation is in agreement with the results presented in fig. 9. Figures 4 and 5 display the effect of β on velocity and temperature profile. From fig. 4 it is noticed that ferromagnetic interaction parameter β illustrate the effect of the external magnetic field induced by the magnetic dipole on the dynamics of the fluid. The presence of magnetic field β acts as increases so does the retarding force and hence the axial velocity decreases as shown in fig. 4, whereas reverse trend exhibited for temperature profile as seen

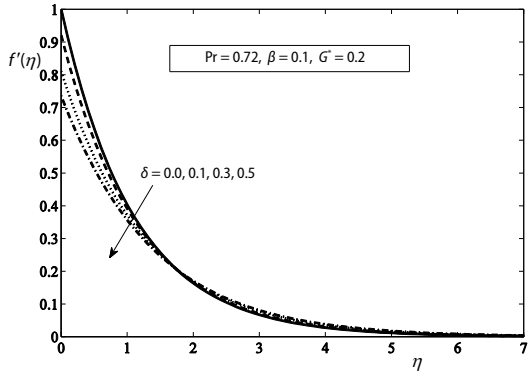

Figure 2. Effect of slip parameter δ on velocity profile *vs.* η

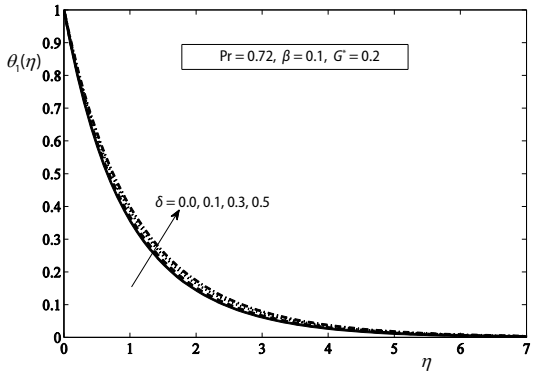

Figure 3. Effect of slip parameter δ on temperature profile *vs.* η

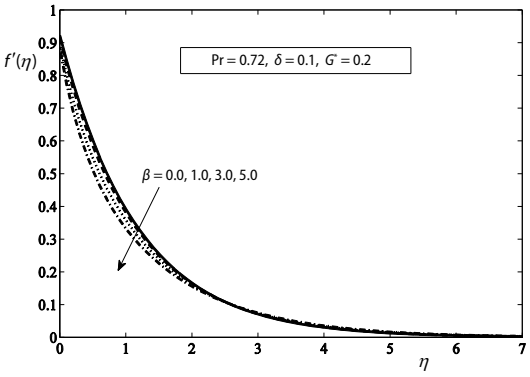

Figure 4. Effect of ferromagnetic interaction parameter β on velocity profile *vs.* η

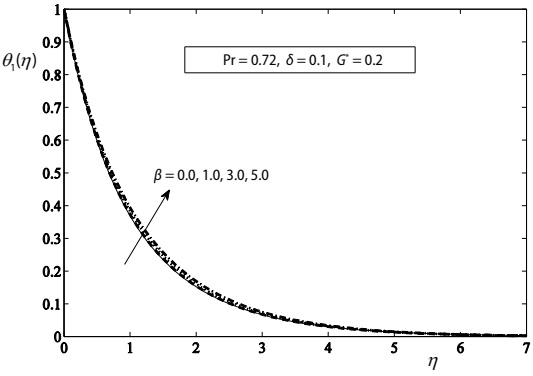

Figure 5. Effect of ferromagnetic interaction on β temperature profile *vs.* η

in fig. 5. Figure 6 illustrate the variation of buoyancy parameter G^* on $f'(\eta)$. It is noted that velocity f' increases when G^* increases. The boundary layer thickness also increases for large value of G^*. Figure 7 depict the variations of G^* on $\theta(\eta)$. It is evident from these figures that an increase in the buoyancy parameter results in a decrease in the thermal boundary layer thickness. Figure 8 represent the graph of temperature profile for different values of Prandtl number. From the fig. 8 it is seen that the effect of Prandtl number is to decrease the temperature, which results in decrease of the thermal boundary layer thickness with the increase of values of Prandtl number. The increase of Prandtl number means slow rate of thermal diffusion. Figures 9 and 10 shows the local skin friction coefficient and Nusselt number with the variation of β for different values of slip parameter δ. It is observed in the fig. 9 that the skin friction coefficient increases with the variation of β, whereas it decreases with velocity slip parameter δ. It means that in the no-slip velocity condition ($\delta = 0.0$) the highest surface shear stress occurs for ferro fluid ($\beta = 0$). Figure 10 shows the heat transfer rate with β for different values of velocity slip parameter δ. From figure it can be seen that heat transfer rate decreases for both β as well as slip parameter δ. Figure 11 display the pressure profile with the variation of β for different valued of slip parameter δ. From the figure it is noticed that pressure is increases for the variation of β as well as slip parameter δ. Figures 12-14 are plotted for Nusselt number,

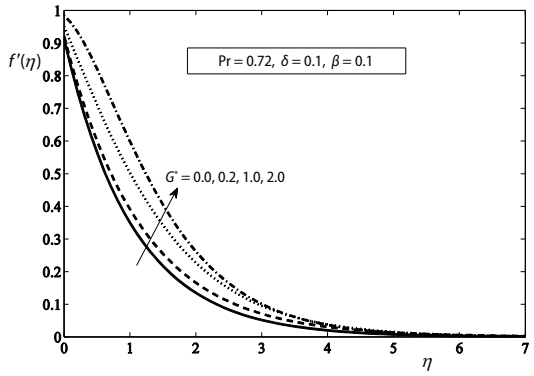

Figure 6. Effect of Buoyancy parameter G^* on velocity profile *vs.* η

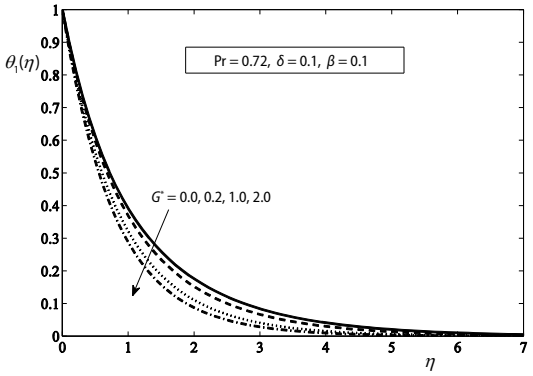

Figure 7. Effect of Buoyancy parameter G^* on temperature profile *vs.* η

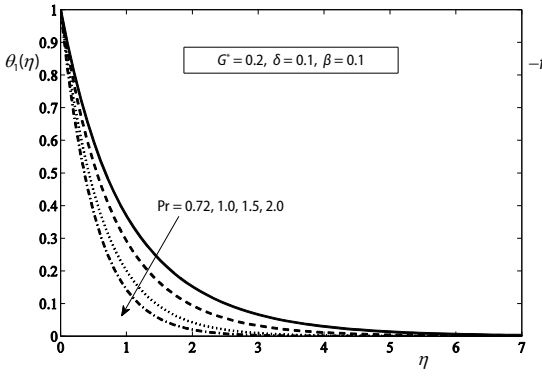

Figure 8. Effect of Prandtl number Pr on temperature profile *vs.* η

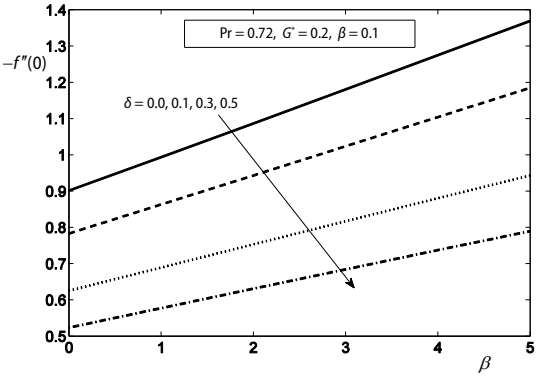

Figure 9. Effect of slip parameter δ on local skin friction coefficient with the variation of ferromagnetic interaction parameter β

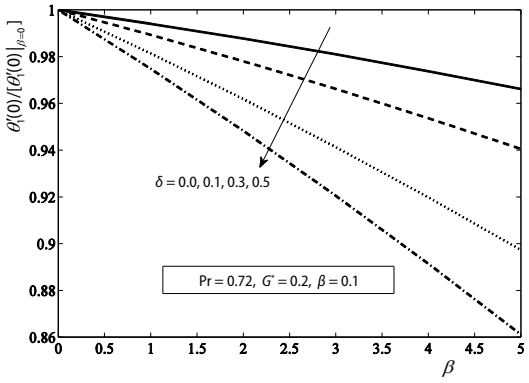

Figure 10. Effect of slip parameter δ on Nusselt number with the variation of ferromagnetic interaction parameter β

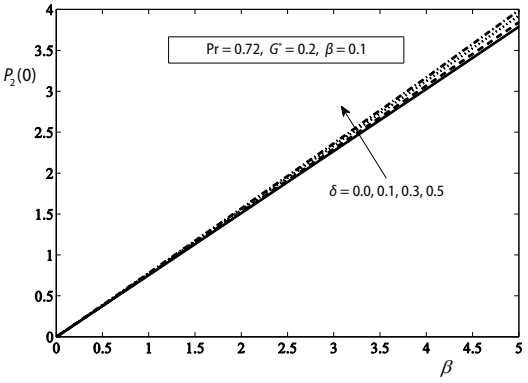

Figure 11. Effect of slip parameter δ on pressure with the variation of ferromagnetic interaction parameter β

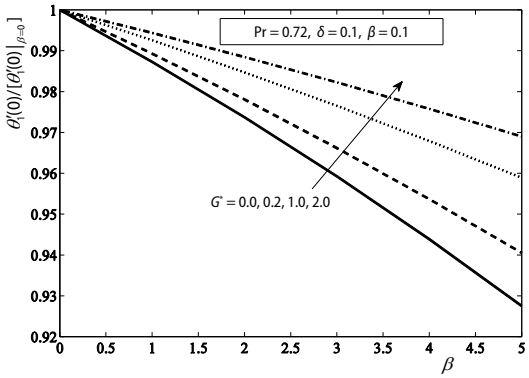

Figure 12. Effect of G^* on Nusselt number with the variation of ferromagnetic interaction parameter β

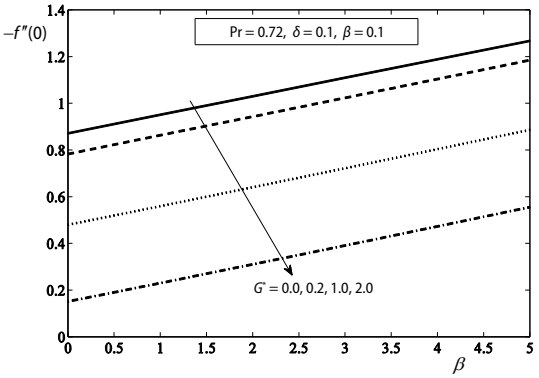

Figure 13. Effect of G^* on local skin friction with the variation of ferromagnetic interaction parameter β

local skin friction and pressure with the variation of β for different values of buoyancy parameter G^*. From fig. 12 it is observed that Nusselt number is decreases with the variation of β, whereas it increases with buoyancy parameter G^*. Figure 13 show that local skin friction coefficient increases with the variation of β, whereas reverse trend is occur for different values of G^*. Figure 14 display the pressure for different values of buoyancy parameter. From figure it is reveals that pressure is decreases with an increase in G^*, whereas linearly increasing with the variation of β.

To validate the accuracy of present method, the values of heat transfer coefficient $\theta_1'(0)$

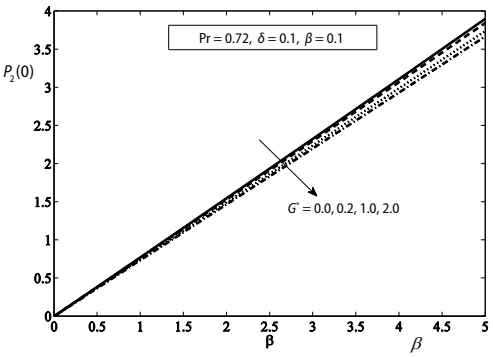

Figure 14. Effect of G^* on pressure with the variation of ferromagnetic interaction parameter β

are compared with the results reported by Chen [46], Abel *et al*. [47] and Ali [48] for various values of Prandtl number in the absence of ferromagnetic interaction parameter as shown in tab. 1. An excellent agreement with the existing results can be easily observed from it. Further tab. 2 displays the values of local skin-friction and local, heat transfer rate in the presence of β.

Table 1. Comparison of surface temperature gradient $-\theta_1'(0)$ for different values of Pr when $G^* = \beta = \delta = \lambda = 0$

Pr	Chen [46]	Abdel *et al*. [47]	Ali [48]	Present work
0.72	1.0885	1.0885	…	1.08863
1	1.3333	1.3333	1.3333	1.3334
3	2.5097	…	2.5097	2.50967
10	4.7968	4.7968	4.7968	4.79671

Table 2. Values of local skin friction coefficient $-f''(0)$ and temperature gradient $-\theta_1'(0)$ for different values of β when Pr = 1

β	$-f''(0)$	$-\theta_1'(0)$
0.0	1.0000	1.3333
0.5	1.0507	1.3286
1.0	1.1015	1.3237
0.3	1.1524	1.3187

Concluding remarks

In this paper the problem of 2-D viscous and incompressible ferrofluid flow over a stretching sheet with the effect of buoyancy parameter and partial slip boundary condition was studied. The governing partial differential equations for mass, momentum, and energy were transformed into ordinary differential equations using a similarity transformation. These equations were solved numerically using shooting method with Runge-Kutta Fehlberg fourth-order scheme. The effects of various physical parameters like ferromagnetic interaction parameter, β, buoyancy parameter, G^*, velocity slip parameter, δ, and Prandtl number, Pr, on velocity and temperature profiles are shown graphically and discussed. Some of the major finding in our analysis are as follows.

- Velocity $f'(\eta)$ increases with G^* and decreases when δ and β increases.
- Temperature profiles increases for δ and β whereas it decreases with G^* and Prandtl number.
- Nusselt number is decreasing for δ and increasing for G^*.
- Local skin friction coefficient decreases when δ and G^* increases with the variation of ferromagnetic interaction parameter β.

Nomenclature

a – distance, [m]
C_{fx} – skin friction coefficient, [–]
c_p – specific heat transfer, [Jkg^{-1}K^{-1}]
G^* – mixed convection parameter
Gr_x – local Grashof number, [–]
H – magnetic field, [Am^{-1}]
K^* – pyromagnetic coefficient
k – thermal conductivity, [Wm^{-1}K^{-1}]
M – magnetization, [Am^{-1}]
Nu_x – local Nusselt number, [–]
Pr – Prandtl number, [–]
T_c – Curie temperature, [K]
u, v – velocity components, [ms^{-1}]
x, y – Cartesian component, [m]

Greek Symbols

α_1 – dimensionless distance, [–]
β – ferromagnetic interaction parameter
γ – magnetic field strength, [Am^{-1}]
δ – velocity slip parameter
ε – dimensionless Curie temperature, [–]
λ – viscous dissipation parameter
ρ – density, [kgm^{-3}]
τ_w – shear stress
ϕ – magnetic potential
ψ – stream function, [m^{2}s^{-1}]

References

[1] Crane, L. J., Flow Past a Stretching Plate, *J. Appl. Math. Phys., 21* (1970), 4, pp. 645-647
[2] Gupta, P. S., Gupta, A. S., Heat and Mass Transfer on a Stretching Sheet with Suction or Blowing, *The Canadian Journal of Chemical Engineering, 55* (1977), 6, pp. 744-746

[3] Grubka, L. J., Bobba, K. M., Heat Transfer Characteristics of a Continuous, Stretching Surface with Variable Temperature, *Journal of Heat Transfer, 107* (1985), 1, pp. 248-250
[4] Vafai, *et al*., The Study of Hall Current on Peristaltic Motion of a Non-Newtonian Fluid with Heat Transfer and Wall Properties, *Zeitschrift fuer Naturforschung A, 70* (2015), 4, pp. 281-293
[5] Ellahi, R., *et al.,* Non-Newtonian Fluid Flow through a Porous Medium between Two Coaxial Cylinders with Heat Transfer and Variable Viscosity, *Journal of Porous Media, 16* (2013), 3, pp. 205-216
[6] Ellahi, R., The Effects of MHD and Temperature Dependent Viscosity on the Flow of Non-Newtonian Nanofluid in a Pipe: Analytical Solutions, *Applied Mathematical Modeling, 37* (2013), 3, pp. 1451-1457
[7] Salama, F. A., Effects of Radiation on Convection Heat Transfer of Cu-Water Nanofluid Past a Moving Wedge, *Thermal Science*, *20* (2016), 2, pp. 437-447
[8] Moradi, A., *et al.,* Investigation of Heat Transfer and Viscous Dissipation Effects on the Jeffery Hamel Flow of Nanofluids, *Thermal Science,* 19 *(*2015), 2, pp. 563-578
[9] Kandelousi, M. S., Effect of Spatially Variable Magnetic Field on Ferrofluid Flow and Heat Transfer Considering Constant Heat Flux Boundary Condition, *The European Physical Journal Plus*, *129* (2014), Nov., 248
[10] Kandelousi, M. S., KKL Correlation for Simulation of Nanofluid Flow and Heat Transfer in a Permeable Channel, *Physics Letters A*, *378* (2014), 45, pp. 3331-3339
[11] Sheikholeslami, *et al.,* Convection of Al_2O_3-Water Nanofluid Considering Thermal Radiation: A Numerical Study, *International Journal of Heat and Mass Transfer*, *96* (2016), May, pp. 513-524
[12] Mohyud-Din, *et al.,* Magnetohydrodynamic Flow and Heat Transfer of Nanofluids in Stretchable Convergent/Divergent Channels, *Applied Sciences*, *5* (2015), Nov., pp. 1639-1664
[13] Mohyud-Din, *et al.,* On Heat and Mass Transfer Analysis for the Flow of a Nanofluid between Rotating Parallel Plates, *Aerospace Science and Technology*, *46* (2015), Oct.-Nov., pp. 514-522
[14] Rashidi, M. M., *et al.,* Entropy Generation Analysis of the Revised Cheng-Minkowycz Problem for Natural Convective Boundary Layer Flow of Nanofluid in a Porous Medium, *Thermal Science*, *19* (2015), Suppl. 1, pp. S169-S178
[15] Ellahi, R., *et al.*, A Study of Heat Transfer in Power Law Nanofluid, *Thermal Science, 20* (2016), 6, pp. 2015-2026
[16] Hathway, D. B., Use of Ferrofluid in Moving Coil Loudspeakers dB-Sound *Engg. Mag., 13* (1979), pp. 42-44
[17] Raj, K., Moskowitz, R., Commercial Applications of Ferrofluids, *J. Magn. Mater., 85* (1990), 1-3, pp. 233-245
[18] Ellahi, R., *et al.*, Effects of MHD and Slip on Heat Transfer Boundary Layer Flow over a Moving Plate Based on Specific Entropy Generation, *Journal of Taibah University for Science, 12* (2018), 4, pp. 476-482
[19] Shliomis, M. I., Ferrofluids as Thermal Ratchets, *Physical Review Letters, 92* (2004), 18, 188901
[20] Maruno, S., *et al*., Plain Paper Recording Process Using Magnetic Fluids, *J. Mgn. Magn. Mater., 39* (1983), 1-2, pp. 187-189
[21] Rosensweig, R. E., Ferrohydrodynamics, *Cambridge University Press, Cambridge, London,* 1985
[22] Neuringer, J. L., Some Viscous Flows of a Saturated Ferrofluid under the Combined Influence of Thermal and Magnetic Field Gradients, *Int. J. Nonlinear. Mech., 1* (1966), 2, pp. 123-127
[23] Tzirtzilakis, E. E., *et al*., Numerical Study of Forced and Free Convective Boundary Layer Flow of a Magnetic Fluid over a Flat Plate under the Action of a Localized Magnetic Field, *Zeitschrift fuer Angewandte Mathematik und Physik, 61* (2010), 5, pp. 929-947
[24] Sheikholeslami, M., Ellahi, R., Simulation of Ferrofluid Flow for Magnetic Drug Targeting Using Lattice Boltzmann Method, *Journal of Zeitschrift fuer Naturforschung A, 70* (2015), 2, pp. 115-124
[25] Sheikholeslami, M., Gorji-Bandpy, M., Free Convection of Ferrofluid in a Cavity Heated from Below in the Presence of an External Magnetic Field, *Powder Technology, 256* (2014), Apr., pp. 490-498
[26] Li, Q., Xuan, Y., Experimental Investigation on Heat Transfer Characteristics of Magnetic Fluid Flow around a Fine Wire under the Influence of an External Magnetic Field, *Exp. Therm. Fluid. Sci., 33* (2009), 4, pp. 91-596
[27] Motozawa, M., *et al*., Effect of Magnetic Field on Heat Transfer in Rectangular Duct Flow of a Magnetic Fluid, *Phys. Procedia., 9* (2010), June, pp. 190-193
[28] Feng, W. U., *et al*., Acoustically Controlled Heat Transfer of Ferromagnetic Fluid, *International Journal of Heat and Mass Transfer, 44* (2001), 23, pp. 4427-4432
[29] Tangthieng, C., *et al*., Heat Transfer Enhancement in Ferrofluids Subjected to Steady Magnetic Fields, *J. Magn. Magn. Mater., 201* (1999), 13, pp. 252-255

[30] Stiles, P. J., *et al*., Heat Transfer through Ferrofluids as a Function of the Magnetic Field Strength, *J. Colloid Interface. Sci., 155* (1993), 1, pp. 256-258
[31] Abdallah, I. A., Analytical Solution of Heat and Mass Transfer over a Permeable Stretching Plate Affected by a Chemical Reaction, Internal Heating, Dufour-Souret Effect and Hall Effect, *Thermal Science*, *13* (2009), 2, pp. 183-197
[32] Zeeshan, *et al*., Effect of Magnetic Dipole on Viscous Ferrofluid Past a Stretching Surface with Thermal Radiation, *Journal of Molecular Liquids, 215* (2016), Mar., pp. 549-554
[33] Nawaz *et al.*, Joules Heating Effects on Stagnation Point Flow over a Stretching Cylinder by Means of Genetic Algorithm and Nelder-Mead Method, *International Journal for Numerical Methods for Heat and Fluid Flow, 25* (2015), 3, pp. 665-684
[34] Kazem, S., *et al*., Improved Analytical Solutions to a Stagnation-Point Flow Past a Porous Stretching Sheet with Heat Generation, *Journal of the Franklin Institute, 348* (2011), 8, pp. 2044-2058
[35] Hayat, T., *et al*., Slip Flow and Heat Transfer of a Second Grade Fluid Past a Stretching Sheet through a Porous Space, *International Journal of Heat and Mass Transfer, 51* (2008), 17, pp. 4528-4534
[36] Martin, M. J., Boyd, I. D., Momentum and Heat Transfer in a Laminar Boundary Layer with Slip Flow, *J. Thermophys. Heat Transf., 20* (2006), 4, pp. 710-719
[37] Andersson, H. I., Slip Flow Past a Stretching Surface, *Acta. Mechanica., 158* (2002), 1, pp. 121-125
[38] Ali, M. E., The Effect of Variable Viscosity on Mixed Convection Heat Transfer along a Vertical Moving Surface, *International Journal of Thermal Sciences, 45* (2006), 1, pp. 60-69
[39] Hayat, T., *et al*., Heat and Mass Transfer for Soret and Dufour's Effect on Mixed Convection Boundary Layer Flow over a Stretching Vertical Surface in a Porous Medium Filled with a Viscoelastic Fluid, *Communications in Nonlinear Science and Numerical Simulation, 15* (2010), 5, pp. 1183-1196.
[40] Akbar, N. S., *et al.* Influence of Mixed Convection on Blood Flow of Jeffery Fluid through a Tapered Stenosed Artery, *Thermal Science,* 17 (2013), 2, pp. 533-546.
[41] Ellahi, R., *et al*., A Study on the Mixed Convection Boundary Layer Flow and Heat Transfer over a Vertical Slender Cylinder, *Thermal Science, 18* (2014), 4, pp. 1247-1258
[42] Nezhad, A. H., Ardalan, M. V., A New Approach for the Analysis of the Nanoparticles Effects on Cu-Water Nanofluid Mixed Convection Heat Transfer and Required Power in a Lid-Driven Cavity, *Thermal Science*, *20* (2016), 20, pp. 133-139
[43] Mahmoodi, M., Mixed Convection Inside Nanofluid Filled Rectangular Enclosures with Moving Bottom Wall, *Thermal Science, 15* (2011), 3, pp. 889-903
[44] Ellahi, R., *et al*., Shape Effects of Spherical and Nonspherical Nanoparticles in Mixed Convection Flow over a Vertical Stretching Permeable Sheet, *Journal Mechaniss of Advanced Materials and Structures, 24*, (2017), 15, pp. 1231-1238
[45] Andersson, H. I., Valnes, O. A., Flow of a Heated Ferrofluid over a Stretching Sheet in the Presence of a Magnetic Dipole, *Acta Mechanica, 12* (1998), 8, pp. 39-47
[46] Chen, C. H., Laminar Mixed Convection Adjacent to Vertical Continuously Stretching Sheets, *Heat and Mass Transfer, 33* (1998), 5-6, pp. 471-476
[47] Abel, M. S., *et al*., Viscoelastic MHD Flow and Heat Transfer over a Stretching Sheet with Viscous and Ohmic Dissipations, *Communications in Nonlinear Science and Numerical Simulation, 13* (2008) , 9, pp. 1808-1821
[48] Ali, M. E., Heat Transfer Characteristics of a Continuous Stretching Surface, *Waerme-und Stoffuebertragung, 29* (1994), 4, pp. 227-234

Paper submitted: Jun 10, 2016
Paper revised: October 8, 2016
Paper accepted: October 12, 2016